Visualization of Current Sheet Canting in a Pulsed Plasma Accelerator

T.E. Markusic*and E.Y. Choueiri†
Electric Propulsion and Plasma Dynamics Laboratory (EPPDyL)
Mechanical and Aerospace Engineering Department
Princeton University, Princeton, New Jersey 08544

IEPC-99-206‡

Abstract

The formation and propagation of current sheets in a rectangular-geometry pulsed plasma accelerator was observed using high speed cameras equipped with narrow-pass line filters. The objective of this investigation was to determine if any asymmetries or instabilities are present in current sheets which may be detrimental to the performance of pulsed plasma thrusters. Photographs of the light emitted from the current sheet during initiation, propagation, and ejection were acquired. The influence of varying gas species, gas pressure, capacitor bank voltage, and electrode polarity was investigated. The most conspicuous feature of these recorded images is that current sheets propagate with highly canted angles (relative to the electrode normal). Ion conduction current, electrode erosion, magnetic field asymmetry, and the Hall effect are discussed as possible causes of this canting.

1 Introduction

The classical description of the acceleration mechanism in a pulsed plasma thruster (PPT) involves the formation and propagation of a current sheet which entrains gas as it propagates along the acceleration channel, acting as an electromagnetic snowplow[1]. Therefore, a fundamental understanding of why current sheets can fail to maintain good propellant sweeping characteristics is essential to the development of more effective PPTs.

This paper addresses the phenomenon of current sheet canting — the departure of the current sheet from perpendicular attachment to the electrodes to a skew, or tipped attachment. Severe canting, at angles of up to sixty degrees relative to the electrode normal, has been observed in the present study. This canting may have adverse implications for PPT performance; canting may create off-axis components of thrust, which constitute a profile loss. To take corrective action, it is first essential to understand the physical mechanism which causes canting to occur. This paper reports on the first phase of a continuing study; this first phase focuses on visualization and aims to provide a visual foundation for further investigation.

High speed cameras have been used to gain a detailed but qualitative picture of the behavior of current sheets. In the Experiment section of this report, we show how the discharge evolves: initiation, stable propagation, and ejection. Also, the influence of varying gas species and pressure is described. In the Discussion section we review the work of earlier researches, and posit explanations for physical processes which are capable of causing current sheet canting.

2 Apparatus

The first goal of the Current Sheet Stability Experiment (CSSX) was to develop an experimental apparatus in which current sheets could be reproducably generated in a geometry in which the discharge is easily accessible to a host of diagnostic tools. Also, it was desired that the device be amenable to analyt-

*Graduate Student, Air Force Palace Knight. Member AIAA.

†Chief Scientist at EPPDyL. Assistant Professor, Applied Physics Group. Senior Member AIAA.

‡Presented at the 26^{th} International Electric Propulsion Conference, Kitakyushu, JAPAN, October 17-21,1999.

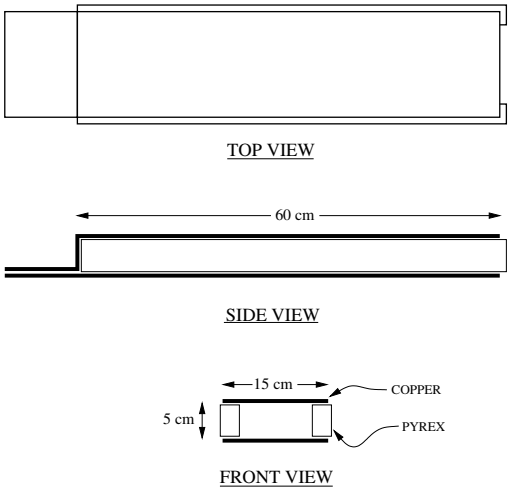

Figure 1: Schematic of CSSX Accelerator I.

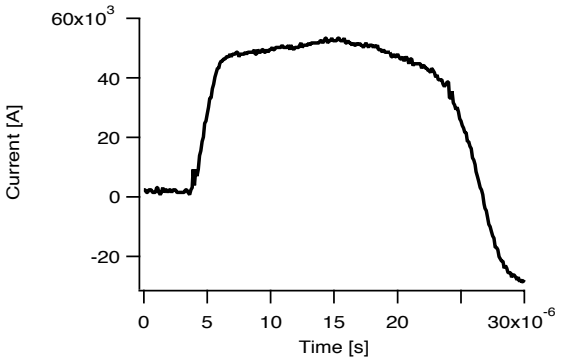

Figure 2: Typical current waveform (propellant: argon (p=100 mTorr) , voltage: 4 kV).

ical analysis; to this end, the design aimed to keep constant as many parameters as possible (e.g., constant current amplitude, uniform gas loading, one-dimensional magnetic and electric fields, etc.). It was decided that a parallel plate geometry best conformed to the design goals.

2.1 CSSX Accelerator I

The CSSX Accelerator I is a parallel plate pulsed plasma accelerator with glass sidewalls (a schematic illustration with relevant dimensions is shown in Fig. 1). The electrodes themselves are made of copper, while the glass sidewalls are made of Pyrex. The sidewalls reduce the region accessible to the discharge to 10 cm (width), whereas the electrodes themselves are 15 cm wide. The motivation for using Pyrex sidewalls is several-fold: first, they provide an excellent optical view of the discharge, second, they isolate the current sheet to a well defined spatial region, third, they isolate the discharge from electric field singularities which are associated with the sharp edges of the electrodes, and lastly, they isolate the discharge from the rapidly fringing magnetic field at the edges of the electrodes. The two latter benefits tend to make the discharge environment more conducive to the formation of spatially uniform current sheets.

The accelerator is powered by an eight stage pulse forming network (PFN). The values of the electrical components at each stage were chosen to give a nearly flat current profile with a pulse width that corresponds to the time it takes the current sheet to traverse the length of the accelerator. Each stage is composed of an 18 μF capacitor in series with a 100 nH inductor. The bank voltage was generally set to 5 kV, yielding a total discharge energy on the order of 2 kJ. The PFN was switched into the accelerator using an ignitron. The peak current was approximately 60 kA, with an initial rise rate on the order of 10^{10} A/s. The duration of each pulse was about 20 μs, which was followed by one cycle of damped ringing. A typical current trace is shown in Fig. 2.

Propellant loading was accomplished using the ambient fill technique. After the vacuum tank was pumped down to its base pressure, the entire tank was brought to the desired operating pressure with the chosen propellant (helium, argon, and xenon were used in the present study). This resulted in a uniform gas distribution within the accelerator prior to discharge initiation.

In general, the apparatus performed very well; current sheets were generated in the expected manner (i.e., formation at the breech and propagation to the exit) and the experiments were very repeatable.

2.2 High speed cameras

Two cameras were used in this experiment: one that can take many pictures in a single experimental run at a very fast framing rate, and a second which can take only one frame per run, but with a very short exposure time. The first, a Hadland Photonics Imacon 792LC, is capable of taking pictures at a rate of up to 20 MHz and provides up to sixteen images printed on Polaroid film. In the experiments presented here, the framing rate was set to 500 kHz; the exposure time for each image was 400 ns. This camera was useful for

creating movies which show how the discharge evolves spatially during the entire pulse. When resolution of finer spatial structure was desired, the second camera, a Princeton Instruments ICCD 576 camera was used. This intensified camera captured single frames onto a 576×384 CCD array with exposure times as low as 10 ns.

2.3 Vacuum facility

The vacuum facility used in this experiment is described in detail by Jahn [2]. The vacuum vessel is a 1 m diameter, 2 m long cylindrical tank made entirely of Plexiglass (which has been shown to eliminate the (unwanted) electromagnetic interactions sometimes found in metallic vessels), with glass optical access windows. Gases are introduced into the tank using a regulated feed-through. The tank uses a diffusion pump with a freon-cooled trap to achieve a base pressure of 4×10^{-5} Torr. Sub-milliTorr pressures are measured with a CVC cold cathode gauge. All pressures above one milliTorr are monitored using a Granville-Phillips 275 Convectron gauge.

3 Experiment

The goal of the CSSX visualization experiments was to verify that the CSSX Accelerator I was indeed generating current sheets and to get a qualitative feel for the type of macroscopic arc structure that evolves during the discharge. The first photographs revealed severely canted current sheets; consequently we turned our attention to understanding this phenomenon. The influence of pressure and gas species on canting was explored. In the subsections below, the photographic record of these experiments is presented.

3.1 Nature of emitted radiation

In order to interpret photographic information it is first necessary to characterize the nature of the radiation which is being emitted by the discharge, i.e., to define whether the radiation is broadband or line, whether the source of radiation is propellant or erosion products, etc.. This is important, for example, if the output of narrow pass optical filters is to be trusted as representative of the species for which the filter is designed to isolate.

As a representative case, the emission spectrum of a 150 mTorr argon accelerator discharge (3 kV bank voltage) from 400-750 nm was acquired using a 0.75 m spectrometer. The spectra were recorded by the ICCD 576 camera described in section 2.2. The spatial location of the measurement was in the mid-plane of the discharge (halfway between the anode and cathode). The camera was exposed for 110 ns, about 10 μs into the current pulse. The resulting spectrum shows that line radiation from excited argon ion and neutrals dominates. Also, copper (from the electrodes) lines were absent.

3.2 Evolution of the the discharge

The Imacon camera was used to obtain spatially and temporally resolved images of a single discharge event; the interframe delay of the Imacon was set to 2 μs. If the initiation of the discharge is offset by 1 μs, the good reproducibility of the discharge structure allows two separate runs to be interlaced to give a succession of images that shows the complete discharge event in 1 μs intervals — the formation of the current sheet, propagation, and ejection from the exit.

Figure 3 shows photographs of a discharge for several successive times during a single pulse (the times shown correspond to those in the current waveform of Fig. 2). The Polaroid images were scanned into a computer and processed with photo-editing software. Lines were drawn to indicate the position of the electrodes. The two vertical rectangles on the electrodes represent bolts that are used to hold the accelerator together; they caused an optical obstruction between the plasma and the camera. The top electrode is the anode. The propellant used was argon at 100 mTorr and the capacitor bank voltage was set to 4 kV. A narrow-pass line filter (488 nm, 10 nm FWHM) was used to allow only the light emitted by argon ions to enter the camera; this was done to exclude the more diffuse glow of the neutrals, and enhance the contrast in the regions where current was flowing.

The photographs show that the discharge forms at the breech, accelerates down the electrodes, and is ejected from the exit. Immediately after the current sheet leaves the breech it begins to tilt — with the anode attachment leading that of the cathode. The sheet then stabilizes to a fairly fixed angle, leaving a trail of plasma along the cathode in its wake, while it propagates down the rest of the discharge channel. Since the anode arc attachment reaches the end of the accelerator first, the ejection of the plasma is quite asymmetric; the current sheet is forced to curl back on itself to re-attach at the anode.

The discharge propagates 60 cm in approximately

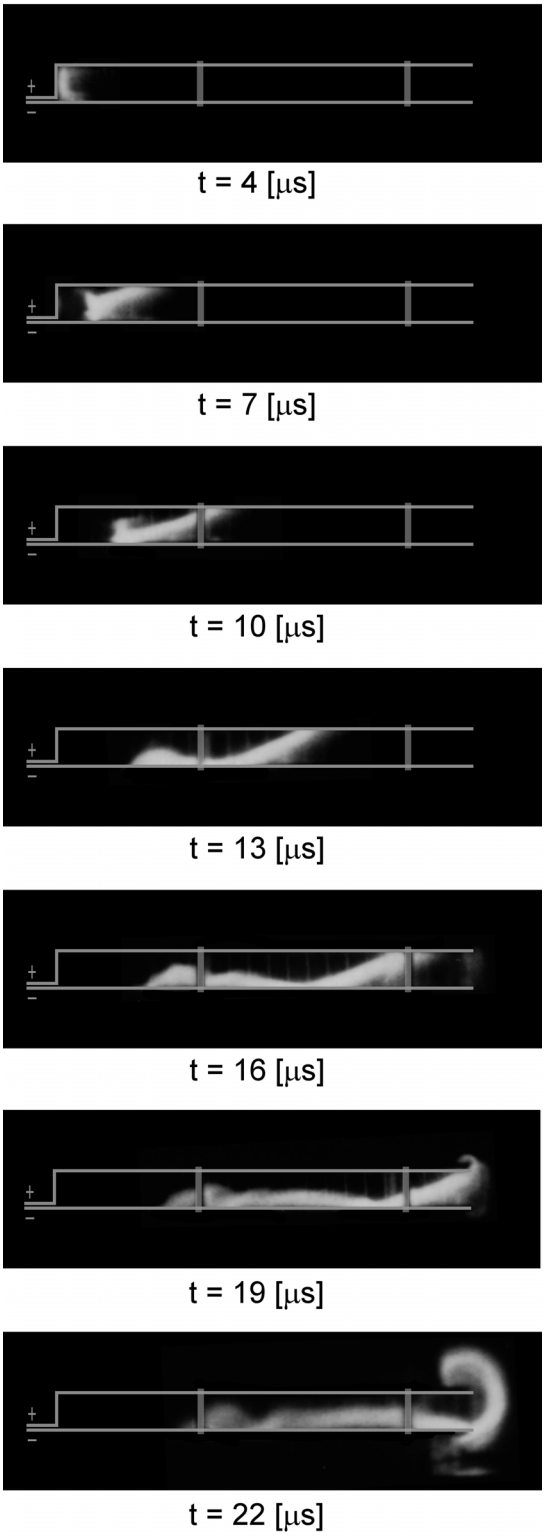

Figure 3: Series of photographs showing the evolution of the discharge in a single pulse (p=100 mTorr (argon), V = 4 kV).

15 μs inferring an average sheet speed of about 4 cm/μs.

Figure 5 shows a close-up of the breech region of the accelerator. The initial conditions for the accelerator in this set of photographs was the same as those used in Fig. 3, with the exception that the bank voltage was 5 kV instead of 4 kV. This figure more clearly shows the transition of the arc from its planar initial state, to the fully canted current sheet. As the current sheet leaves the back of the accelerator, it immediately begins to bifurcate. The initial anode attachment point recedes from the electrode, and a diagonal sheet forms. Within several microseconds the sheet attains the canted structure that it maintains for the remainder of its propagation. The base of the arc (cathode attachment) forms a hook-like structure which has been previously reported in studies of z-pinch accelerators [3].

In the very early stages of the discharge many filamentary structures are visible. Figure 4 shows two pictures, from separate discharges, during the first several hundred nanoseconds of current flow. Argon (100 mTorr) was used; the bank voltage was set to 5 kV. The lower image was acquired at a slightly later time than the upper image. The luminous structure parallel to the electrodes shown to be evolving in the top panel of Fig. 4 are typical of breakdown waves, commonly known as streamers.

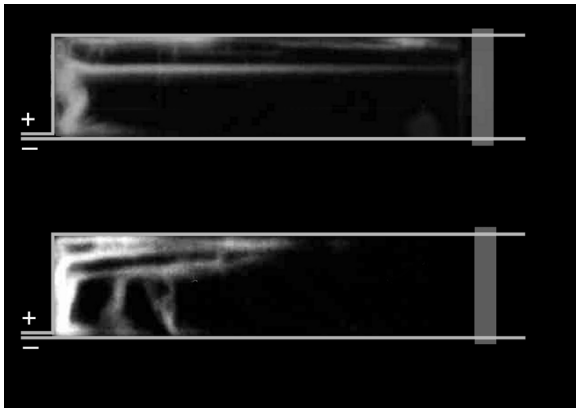

Figure 4: Two images from the initiation stage (first few hundred nanoseconds) of the discharge (p=100 mTorr (Argon), V=5 kV).

3.3 Parametric study

The free parameters in this study were capacitor bank voltage, gas pressure, and gas species. These parameters were varied in an effort to obtain some preliminary clues for understanding of the nature and causes of current sheet canting.

Polarity of the electrodes. The first operating condition that was changed was the polarity of the electrodes. There was some concern that the asymmetric construction of the back of the accelerator (see Fig. 1) was creating a non-uniform magnetic field behind the current sheet, causing it to tilt. If magnetic field asymmetry is the dominant mechanism which drives the canting, reversing the polarity of the electrodes should not affect the structure of the discharge (i.e., the discharge attachment on the top electrode should still lead the attachment point on the bottom electrode). However, as is apparent in Fig. 6, changing the polarity was found to result in the bottom electrode attachment point leading the top. Gas loading, etc., was identical to the experiment represented in Fig. 3. The conclusions which can be drawn are: it is unlikely that aspects peculiar to the construction of the accelerator are responsible for the canting and, comparing Fig. 3 and Fig. 6, the current sheet always cants such that the anode arc attachment point leads the cathode attachment point.

Capacitor bank voltage. The next parameter that was investigated was the capacitor bank voltage — all other operational conditions were held constant. Changing the bank voltage changes the current rise rate and peak current, so it is not unreasonable to expect that there might be some observable differences in the discharges. Again, argon (100 mTorr) was used. Figure 7 shows two different discharges: one at 2 kV, the other, 5 kV. The pictures were taken at two different times (t=10 μs and t=6 μs, respectively), so that the current sheet profiles could be compared at the same spatial location. Comparison of the two pictures reveals that changing the bank voltage has no noticeable effect on the canting angle. The two discharges look very similar; the lower voltage picture looks slightly more diffuse, lacking the sharp hook on the cathode attachment point that is found in the higher voltage discharge.

Gas pressure. Next, the influence of varying the gas pressure was explored. Figure 8 shows argon discharges at three different pressures. The capacitor bank voltage was 4 kV for all three experiments. The peak current was observed to remain constant (within 2 kA) over the pressure range surveyed. The pictures were all taken at the same time in their respective

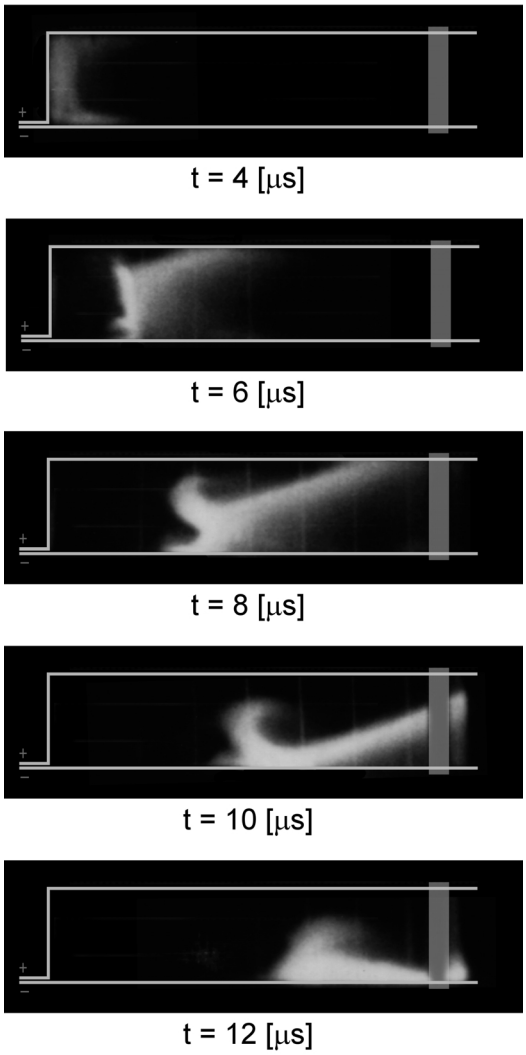

Figure 5: Series of photographs showing the evolution of the discharge near the breech (p=100 mTorr (Argon), V=5 kV).

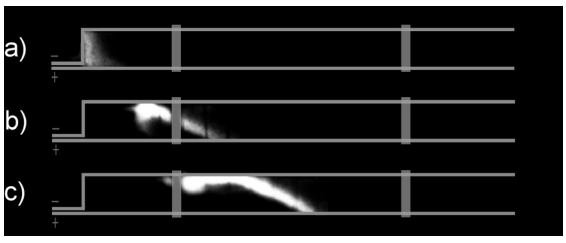

Figure 6: Photographs showing the influence of changing polarity (p=100 mTorr (Argon), V=4 kV): a) t=5μs, b) t=11μs, c) t=14μs.

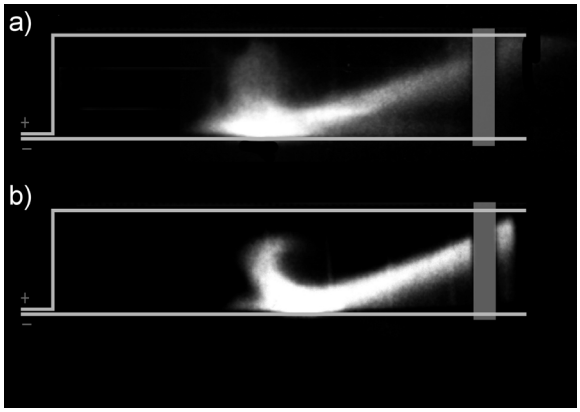

Figure 7: Photographs showing the influence of changing capacitor bank voltage (p=100 mTorr (Argon): a) 2 kV (t=10 μs), b) 5 kV (t=6 μs).

current waveforms.

The figure shows that as pressure is increased the forward motion of the plasma is impeded by the higher mass loading; consequently, the speed of the higher pressure sheet is lower ($v \approx 5$ cm/μs for 50 mTorr, $v \approx 1$ cm/μs for 500 mTorr). Also, at higher pressures the current channel becomes much broader. However, even in the high pressure case we can see vestiges of the lower pressure structure — bifurcation and a canted front. Although at higher pressures the discharge is not appropriately described as a sheet, we can make the observation that the leading edge of the accelerator discharge shows less canting at higher pressures. Just as in the lower pressure cases presented earlier, after the initial transient, the higher pressure discharge was observed to maintain the structure pictured above for the duration of its propagation.

Gas species. Lastly, experiments were conducted using two additional gas species: helium and xenon. Figure 9 shows photographs taken at the same time in their respective current waveforms. The pressure for all three discharges was 100 mTorr. The bank voltage was 4 kV. The peak current in all of the discharges was approximately the same — about 58 kA.

A few qualitative features are apparent in Fig. 9. First, as expected, sheet propagation speed decreases with increasing atomic mass. The helium discharge propagates at approximately 6 cm/μs, and 4 cm/μs in argon. The helium current sheet speed is slower than one would expect from mass loading considerations alone. The xenon discharge has no clear propagation

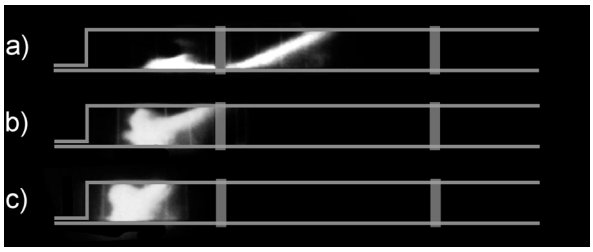

Figure 8: Photographs showing the influence of changing gas pressure (argon, V=4 kV, t=11 μs): a) p=50 mTorr, b) p=240 mTorr, c) p=500 mTorr.

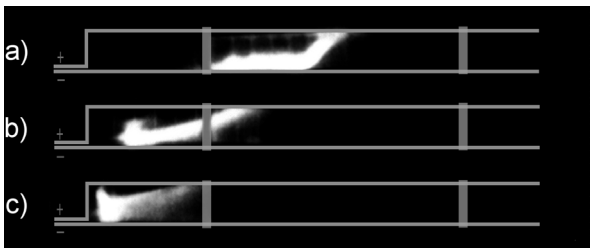

Figure 9: Photographs showing discharges in three different gases (p=100 mTorr, V=4 kV, t=11 μs): a) helium, b) argon, c) xenon.

speed. The discharge anchors itself at the breech; later stages of the discharge are characterized by a bright region near the breech and long filaments of current which extend to the exit, directed nearly parallel to the electrodes. This description of the xenon discharge, along with the comparative photographs of Fig. 9, may indicate a trend of lower current sheet canting angles for lower atomic mass propellants. Experiments with additional gases are needed to validate this assertion.

4 Discussion and Conclusions

This paper presents an array of photographic records of propagating current sheets in a parallel plate accelerator. These photographs show that current sheets may be severely canted in operational regimes that are of propulsive interest. The phenomenon of current sheet canting has been observed by many earlier researchers[4, 5, 3, 6, 7]; however, to our knowledge, no one has systematically attempted to isolate the physical process which drives it. This work repre-

sents the first phase of our long term effort to understand the problem, and ultimately provide design prescriptions to alleviate its negative impact on pulsed plasma thruster performance.

There are several possible explanations for the cause of the canting: unbalanced mass accumulation at the cathode due to ion conduction current, mass accumulation at the cathode due to erosion products, asymmetries in the magnetic field, and the Hall effect. We will now discuss each of these possibilities in turn, and comment on how the limited experimental evidence that our photographic survey has produced supports or contradicts each model.

Ion conduction. Lovberg[5] proposed that if the ion gyroradius becomes large (comparable to the device dimensions) a large number of ion gyro-orbits will intersect the cathode and become slow neutrals. The photographic record provides possible support for such a scenario. Figures 3, 8, and 9 show extensive trails of plasma that are left in the wake of the current sheet, along the cathode. This accumulation of plasma along the cathode may be related to Lovberg's ion conduction current model.

Erosion. Another way that mass could be accumulated along the cathode is through erosion of the electrode material. Our experiments do not support this hypothesis. The spectral survey revealed no evidence of copper in the discharge plasma. Also, a narrow pass filter was mounted on the PI CCD camera to image one of the helium discharges. However, the bandpass of this filter corresponded to a strong copper ion emission line, with no helium lines in the vicinity. The resulting images were completely blank, indicating no substantial population copper emitters.

Asymmetries. Asymmetries in the magnetic field structure may have a strong perturbative influence in pulsed plasma accelerators [8]; however, although asymmetries were almost certainly present in the our experiment, we have shown that the sense of current sheet canting (i.e., the fact that the anode attachment always leads) is much more closely tied to polarity in our device.

Hall effect. The last possibility that we are exploring is the Hall effect. Redding [6] speculated that the Hall effect was responsible for canting in his plate accelerator. The plasma regime in which the CSSX accelerator operates is likely to be influenced by finite Larmor radius effects notwithstanding the Hall effect and plasma turbulence. Rough initial estimates of the electron Hall parameter in our operational regime indicate a value of order unity. This implies a concomitant axial conduction current. Figure 5 indicates that the transient tipping of the current sheet is strongly related to the temporal behavior of the current (which drives the magnetic field). The sheet starts planar (when the current is low), goes through a transient tipping phase (when the current is rapidly rising), and stabilizes to a constant angle for the duration of its propagation (when the current is constant). The fact that the temporal behavior of the tipping of the current sheet is in phase with the temporal evolution of the magnetic field may indicate that the rising magnetic field is driving an increase in the electron gyrofrequency, and hence the Hall parameter, until the steady current magnetic field is achieved. Also, the photographs in Fig. 8 indicate a steepening (less canting) of the current sheet at higher pressures. This is consistent with the Hall effect hypothesis; higher pressures result in higher electron collision frequencies and a lower Hall parameter. As an aside, this may be an indication that current sheet canting is not as much of an issue for pulsed plasma thrusters which operate at higher pressures.

The present investigation has not yielded any conclusive evidence for the origin of current sheet canting. However, it has given us a clear macroscopic view of how the discharge evolves, and indicated directions for future diagnostics. Our immediate plans are to apply the Schlieren photography technique using a rapidly pulsed laser to obtain better spatial resolution of the current channels. Also, we are developing a forty-probe planar array of B-dot probes to give a detailed picture of the the spatial and temporal evolution of the magnetic field during the transient tipping phase of the discharge.

References

[1] R.G. Jahn. *Physics of Electric Propulsion*. McGraw-Hill Book Company, 1968.

[2] R.G. Jahn and K.E. Clark. A large dielecteic vacuum facility. *AIAA Journal*, 1966.

[3] R.L. Burton. *Structure of the Current Sheet in a Pinch Discharge*. PhD thesis, Princeton University, 1966.

[4] R.H. Lovberg. Investigation of current sheet microstructure. *AIAA Journal*, pages 187–198, 1966.

[5] R.H. Lovberg. The measurement of plasma density in a rail accelerator by means of schlieren photography. *IEEE Transactions on Nuclear Science*, pages 1215–1222, 1964.

[6] E. Robert and L. Reding. Etude experimentale d'un accelerateur de plasma a electrodes lineaires. *ONRA Report*, 1968.

[7] Motion and Structure of a Plasma Produced in a Rail Spark Gap. Structure of a large-radius pinch discharge. *AIAA Research Notes*, 1963.

[8] R.G. Jahn and W. von Jaskowsy. Structure of a large-radius pinch discharge. *AIAA Journal*, 1:1809–1814, 1963.